

Optimal Estimation of Several Linear Parameters in the Presence of Lorentzian Thermal Noise

Jason H. Steffen*

Fermilab Center for Particle Astrophysics

Michael W. Moore and Paul E. Boynton

University of Washington, Department of Physics

(Dated: March 3, 2019)

In a previous article we developed an approach to the optimal (minimum variance, unbiased) statistical estimation technique for the equilibrium displacement of a damped, harmonic oscillator in the presence of thermal noise. Here, we expand that work to include the optimal estimation of several, linear parameters for a continuous time series. We show that working in the basis of the thermal driving force both simplifies the calculations and provides additional insight into why estimation techniques that are employed in practice perform as they do. To illustrate this point, we compare the variances in the optimal estimators that we derive for thermal noise with those of two approximate methods which, like the optimal estimators, suppress the contribution to the variance that comes from the unwanted, resonant motion of the oscillator. We discuss how these methods fare when the dominant noise process is either white displacement noise, a regime where the optimal estimators for thermal noise have infinite variance, or noise where the noise power is inversely proportional to the frequency ($1/f$ noise), which is common in modern torsion pendulum experiments. A method to transform a parameter estimating function between the displacement basis and the basis of the thermal driving force is shown for the case of a high- Q oscillator. To find the optimal estimators, we derive and use a generalization of traditional matrix methods for parameter estimation that can accommodate continuous data. A result of this derivation is that the optimal parameter estimators for a multiparameter fit are linear combinations of the optimal estimators that one would obtain for single-parameter fits. We discuss how our results may help refine the design of experiments as they allow an exact, numerical comparison of the precision of estimated parameters under various data acquisition and data analysis strategies.

PACS numbers: 02.50, 02.60

Keywords: Data Analysis, Thermal Noise, Torsion Device

I. INTRODUCTION

After more than two centuries, the principle of the torsion pendulum still underlies the design of instruments to measure ultra-small electrical or gravitational torques. Recent advances in the performance of these devices depend primarily on improvements in electronic readout systems and the care taken to make optimal or near optimal statistical inference considerations the basis for design of both hardware and measurement protocol [1, 2]. The current state of this art is driven by inevitable demands for experimental precision to approach the fundamental limit posed by thermal noise as expressed by the fluctuation-dissipation theorem. In a previous article we developed an approach to the optimal (minimum variance, unbiased) statistical estimation technique for the equilibrium displacement of a damped, harmonic oscillator in the presence of thermal noise (Moore et al. [3], hereafter Paper I).

While that work introduces a useful theoretical treatment and some interesting conclusions, its scope is quite limited because it addresses only the case of a single, linear parameter. For a torsion pendulum under the in-

fluence of an external torque this single parameter fails to distinguish between the equilibrium displacement of the pendulum mass and its equilibrium displacement in the absence of the external torque. Moreover, a real torsion fiber under load slowly unwinds, also requiring parameterization. Consequently, even without considering pendulum oscillations, a multi-parameter model must be employed.

In this article we expand the work presented in Paper I to include the optimal estimation of several, linear parameters. As in the case of a single linear parameter, we note that traditional methodologies for estimating multiple parameters fail for a high- Q , long-period oscillator in the presence of thermal noise. The problem stems from the fact that the oscillator's response to the thermal bath, which drives the oscillator with equal power at all frequencies, peaks sharply at the resonant frequency. In order to minimize the variance in the displacement parameter estimators one must optimally filter the contribution to the displacement variation from this resonance peak.

Superficially, the issues presented by the resonance peak, the recovery of the signal (an external torque), and the unwinding behavior of the torsion fiber appear straightforward. One might consider treating the noise as white, then address each issue to produce an acceptable measurement approach. First, to remove the effects

*jsteffen AT fnal.gov

of the resonance one could use data from an integer number of oscillation periods as illustrated in Paper I. Second, to break the degeneracy between the orientation of the pendulum mass and its orientation in the absence of the source mass one might modulate the signal. Then by choosing the modulation frequency to be distinct from, but commensurate with the oscillation frequency, and also choosing the duration of the data sample to be an integer number of both the oscillation and signal periods, the orthogonality of the fitted parameters over the measurement interval is maintained.

Finally, in order to account for the secular unwinding behavior of the torsion fiber one could include a few low-order polynomials in the fit to the observations. However, these polynomials are generally not orthogonal to the free oscillation of the pendulum, and consequently yield an estimating function for the signal that is no longer orthogonal to the resonance peak.

At this point it becomes clear that such a casual approach must give way to a proper multiple-parameter fitting scheme that filters the “thermal noise” contribution from the resonance peak. The absence from the literature of explicit techniques for optimal parameter estimation in the analysis of high- Q oscillators in gravity experiments whose precision may approach the limitation posed by thermal noise has motivated our search for a practical solution to this problem.

To set a context for presenting the optimal solution, we discuss two, straightforward, approximate methods that suppress the contribution from the resonance peak to the variances of important model parameters. The first, which we call the trigonometric method, is to fit the data optimally for white noise while including the sine and cosine oscillation amplitude parameters of the pendulum. Doing so ensures that the estimators for the remaining parameters—particularly those that correspond to relevant observables—are immune to the variance contribution from the resonance. The second method, employed by the Eöt-Wash group at the University of Washington, is to pre-filter the data by adding a given realization of pendulum motion to itself displaced by half an oscillation period, thereby eliminating the effects of resonant oscillations to a large extent. These pre-filtered data are then fit optimally for white noise[4].

Both methods remove much of the contribution of the resonance peak to the parameter variances because the associated filter functions, when expressed in the Fourier representation, have a notch with a quadratic minimum at the resonant frequency. They also share the advantage that variances remain finite when white displacement noise is superposed on the thermal noise as is the case in any real experiment. By comparison, the variance of the optimal thermal noise estimators diverge when white noise is present because their displacement estimating functions include Dirac delta functions (see Paper I). The ubiquity of white noise motivates us to include these approximate methods in our discussion because they are the schemes that experimentalists actually employ, and likely will continue to employ in the future.

Since the optimal estimation method is pathological in the presence of white noise, comparing it with approximate methods may appear little more than an interesting exercise since an experiment can never be conducted in this idealized context. However, such results establish a firm lower bound to the variance of a parameter estimator enabling one to weigh the effort required to improve the experimental methods to lower the uncertainty in a measurement against the time necessary to implement such modifications.

Moreover, asking which approximate method is superior in a real experiment brings up matters of judgment. An experimentalist must choose an analysis method and justify the choice in light of many aspects of the experiment at hand. Design questions regarding the advantages of a particular length of a data sample, the most appropriate phase of the modulated signal, or the effect of adding additional parameters to the model, when formulated, can be answered with confidence for the case of white noise. For thermal noise, however, the answers to such questions appear unresolved in the literature. In this paper we set forth a basis for such choices.

The major premise of Paper I is that transforming to the driving-force basis—where the force noise is white—allows one easily to determine the optimal thermal noise filter for a single-parameter fit. Here we extend this idea to multivariate fits, but make a second point that was not emphasized in Paper I: transforming to the driving force basis allows one better to understand the efficacy of these approximate methods. As a result, questions about the choices mentioned above can be readily answered with confidence and precision.

We begin our discussion with a comparison of the single-period optimal thermal noise estimator of the equilibrium displacement (derived in Paper I) with a single-period boxcar estimator because it is the foundation of the two approximate estimation methods. We continue with a comparison of optimal, trigonometric, and Eöt-Wash single-parameter estimators of the equilibrium displacement for various durations of the data sample. Then follows a digression to develop the extension of optimal thermal noise estimators to multi-parameter fits. The basic result is that optimal multi-parameter estimating functions are orthonormal linear combinations of the optimal single-parameter estimating functions derived in Paper I. We are then ready to inter-compare the full, multi-parameter versions of the optimal, trigonometric, and Eöt-Wash methods for a modulated signal while fitting constant and linear polynomial terms.

Finally, we consider an extension of the thermal noise model that is of particular interest to the torsion pendulum community. In modern, moderately high vacuum torsion pendulum experiments, thermal noise results primarily from torsion fiber internal loss mechanisms. Empirically, the driving-force power spectral density in this case is better approximated by a $1/f$ spectrum rather than the white spectrum of classical dashpot resistance. Although the optimal methods we develop no longer strictly apply, we investigate how the optimal, trigono-

metric, and Eot-Wash methods compare in the presence of $1/f$ noise.

We make two preliminary comments on the presentation and approximations of this work. First, we choose to present concrete examples based on data that reflect relevant choices for sample duration, signal frequency, etc., in order to inform the reader's experimental intuition. Second, because the quality factor, Q , is typically several thousand in today's torsion pendulum experiments, we simplify our calculations by truncating results to leading order in $1/Q$. This differs from Paper I in which some results were presented as exact, closed-form expressions.

II. OPTIMAL ESTIMATOR VS. BOXCAR ESTIMATOR FOR A SINGLE PERIOD

As a point of departure, we first compare two estimators for the equilibrium displacement of the oscillator in the presence of thermal noise, the optimal estimator and the boxcar estimator. The latter, a simple, uniform average of the time-domain data, is optimal for the case of white displacement noise.

A. Linear Single-Parameter Estimates

We recall from Paper I that a general parameter estimate for a continuous time series is given by

$$\hat{p} = \int_{-\infty}^{\infty} e_{\hat{p}}(t) x(t) dt \quad (1)$$

where $x(t)$ is the data, and the estimating function $e_{\hat{p}}(t)$ is obtained by properly normalizing a filter function. We again use the convention that a capital letter (e.g. $X(t)$) represents an ensemble of realizations which are represented by lower case letters (e.g. $x(t)$). The variance of the corresponding parameter estimator, expressed in the Fourier representation, is

$$\text{var}(\hat{P}) = \frac{1}{2} \int_{-\infty}^{\infty} F^2[e_{\hat{p}}(t); \nu] S[\delta X(t); \nu] d\nu \quad (2)$$

where the Fourier energy density (FED) $F^2[e_{\hat{p}}(t); \nu]$ is the square of the Fourier transform of the estimating function and $S[\delta X(t); \nu]$ is the power spectral density (PSD) of the noise ensemble $\delta X(t)$. Our goal is to calculate the parameter estimator variances to leading order in $1/Q$. For thermal noise, the PSD already contains a factor of $1/Q$, and so we need express the estimating functions only to zeroth order in $1/Q$ (that is, we may use the estimating functions that would be suitable for an undamped oscillator).

B. Single Period Optimal Thermal Noise Estimator

In Paper I we find the optimal estimate of the equilibrium displacement of the oscillator in the presence of

thermal noise. To zero-order in $1/Q$, the single-period, optimal estimate is

$$\hat{c}^{op} = x_m + \frac{v_f - v_i}{2\pi\omega_0} \quad (3)$$

where x_m is the time-average position of the oscillator, v_i and v_f are the initial and final velocities of the oscillator, and ω_0 is the (undamped) oscillation frequency. The corresponding estimating function is

$$e_{\hat{c}}^{op}(t) = \frac{\Theta(t; t_i, t_f)}{\tau_0} + \frac{-\delta'(t - t_f) + \delta'(t - t_i)}{2\pi\omega_0}, \quad (4)$$

where τ_0 is the period of the pendulum, $\Theta(t; t_i, t_f) \equiv \theta(t - t_i) - \theta(t - t_f)$ is the boxcar function, and $\delta'(t)$ is the time derivative of the Dirac delta function. We call this estimate a “force-only” estimate because its estimating function is orthogonal to a free-oscillation transient of arbitrary amplitude and phase. That is,

$$\int_{-\infty}^{\infty} e_{\hat{c}}^{op}(t) \cos(\omega_0 t) dt = 0 \quad (5)$$

and

$$\int_{-\infty}^{\infty} e_{\hat{c}}^{op}(t) \sin(\omega_0 t) dt = 0. \quad (6)$$

All such force-only estimators have a weighting function that can be expressed in the driving-force basis. As shown in Paper I, the optimal displacement estimating function for thermal noise is a boxcar in the force basis

$$y_{\hat{c}}^{op} = \frac{\Theta(t; t_i, t_f)}{2\pi m \omega_0} \quad (7)$$

where m is the mass of the oscillator. Since thermal noise looks white in the force basis, the variance of the estimator is readily calculated in the time domain,

$$\begin{aligned} \text{var}(\hat{C}^{op}) &= 2k_B T \xi \int_{-\infty}^{\infty} y^2 dt \\ &= \frac{\sigma^2}{\pi Q_0} \end{aligned} \quad (8)$$

where $\sigma^2 = k_B T / \kappa$ and k_B is the Boltzmann constant, T is the absolute temperature of the thermal bath, and κ is the torsional spring constant.

C. Transforming Between Driving-Force Basis and Displacement Basis

In our previous work we showed that an estimating function in the force basis, $y_{\hat{p}}(t)$, can be transformed into the corresponding displacement basis estimating function by using the transpose equation-of-motion operator Ω^T

$$\begin{aligned} e_{\hat{p}}(t) &= \Omega^T [y_{\hat{p}}(t)] \\ &= \left(m \frac{d^2}{dt^2} - \xi \frac{d}{dt} + \kappa \right) y_{\hat{p}}(t) \end{aligned} \quad (9)$$

where m is the mass of the oscillator and ξ is the damping coefficient. For example, $e_{\hat{c}}^{op}(t)$ was derived from $y_{\hat{c}}^{op}(t)$ by this method. As we compare the results of various estimation techniques we wish to exploit the simplifications that follow from working in the force basis. Doing so requires that we obtain the force basis estimating function from the displacement basis estimating function—the inverse of what we have done before.

A straightforward approach to find $y_{\hat{p}}$ from $e_{\hat{p}}$ is to consider the equation of motion relating the driving force to the time series

$$\begin{aligned}\mathcal{F} &= \Omega[x(t)] \\ &= \left(m \frac{d^2}{dt^2} + \xi \frac{d}{dt} + \kappa \right) x(t)\end{aligned}\quad (10)$$

where Ω is the equation of motion operator. We know from the solution to this differential equation that, to leading order in $1/Q$,

$$\begin{aligned}x(t) &= x_i \cos(\omega_0(t - t_i)) + \frac{v_i}{\omega_0} \sin(\omega_0(t - t_i)) \\ &+ \frac{1}{m\omega_0} \int_t^\infty \mathcal{F}(t') \sin(\omega_0(t' - t)) dt'.\end{aligned}\quad (11)$$

For a high- Q oscillator the equation of motion operator is well approximated by its transpose, $\Omega \simeq \Omega^T$. Thus, by inspection of (9), (10), and (11) we have

$$y_{\hat{p}}(t) = \frac{1}{m\omega_0} \int_t^\infty e_{\hat{p}}(t') \sin(\omega_0(t' - t)) dt' \quad (12)$$

where, because the estimating function must be identically zero outside of the time series, the boundary value terms vanish.

D. Single Period Boxcar

Let us now apply this method to a boxcar estimator (unless otherwise noted the term “boxcar estimator” will hereafter refer to one constructed in the displacement basis). We first calculate the force basis estimating function that corresponds to the boxcar estimator to zeroth order in $1/Q$

$$\begin{aligned}y_{\hat{c}}^{box}(t) &= \frac{1}{m\omega_0} \int_t^\infty \frac{\Theta(t'; -\tau_0/2, \tau_0/2)}{\tau_0} \sin(\omega_0(t' - t)) dt' \\ &= \frac{\Theta(t; -\tau_0/2, \tau_0/2)}{2\pi m\omega_0} (1 + \cos(\omega_0 t)).\end{aligned}\quad (13)$$

The variance in the corresponding parameter estimator is now

$$\begin{aligned}\text{var}(\hat{C}^{box}) &= 2k_B T \xi \int_{-\infty}^\infty y^2 dt \\ &= \left(\frac{3}{2} \right) \frac{\sigma^2}{\pi Q} \\ &= \frac{3}{2} \text{var}(\hat{C}^{op}).\end{aligned}\quad (14)$$

Thus, the penalty for using the boxcar estimator instead of the optimal estimator is a factor of 3/2 increase in the parameter variance.

From (12) it follows that a force-only $e_{\hat{p}}(t)$ which is bounded (that is, never infinite), such as the boxcar, results in a $y_{\hat{p}}(t)$ that is zero and has zero slope at both t_i and t_f . The sinusoidal term in (13) serves to match these boundary conditions. Since the cosine is orthogonal to a constant function over one period, the amplitude of the boxcar must be the same as in the optimum in order for the estimate to be unbiased, and since the average value of cosine squared is 1/2, the variance increases by 50%. Conversely, if one desires the $y_{\hat{p}}(t)$ to have discontinuous jumps at the endpoints, as the optimal estimator does, then the corresponding $e_{\hat{p}}(t)$ must have $\delta'(t)$'s at each end.

III. COMPARISON OF OPTIMAL, TRIGONOMETRIC, AND EÖT-WASH ESTIMATORS

The factor of 3/2 in equation (14) leads one to ask if additional data improves this result and if the variance in the boxcar estimator ultimately converges to the optimal value. It turns out that it does not. Yet, this optimal filter for white displacement noise can be used to construct an estimator that performs much better when thermal noise dominates. Here we derive the limits of the boxcar estimator when used in its basic form to study and develop two estimators, the Eöt-Wash estimator and the trigonometric estimator, which are based upon it. Following that, we compare the performance of these hybrid estimators for the cases of white noise and “mixed noise”, which has both thermal and white noise components.

A. Thermal Noise and Multiple Period Estimators

Following the calculations in Section II B one can show that the variance of the optimal estimator times the duration of the data, τ , is

$$\text{var}(\hat{C}^{op}) \times \tau = \frac{2\sigma^2}{\omega_0 Q_0} = \text{constant}. \quad (15)$$

Thus, for three periods of data, the optimum variance has decreased by a factor of 1/3. Similarly, for three periods of data the variance in the boxcar estimator has decreased by a factor of 1/3. This pattern continues for data that span an integer multiple of oscillation periods. To leading order in $1/Q$ the variance in the boxcar estimator remains a factor of 3/2 larger than the optimum.

The estimator employed by the Eöt-Wash group improves upon this by averaging the time series with itself displaced by 1/2 period. However, doing so requires an additional 1/2 period of raw data. The 3.5-period Eöt-

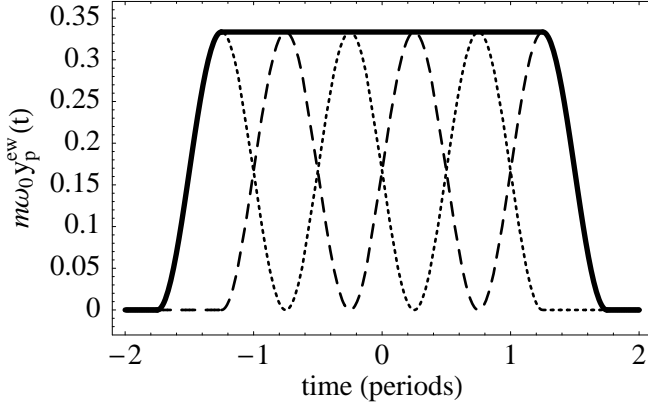


FIG. 1: An example of the Eöt-Wash estimating function. The two dashed curves correspond to the data and the data displaced by half of one oscillation period. Their sum, the Eöt-Wash estimating function, is the solid curve. Note that the sinusoidal terms contribute only near the ends of the observation interval, allowing the variance in the equilibrium displacement estimator to approach the optimal value as the duration of the data increases.

Wash estimating function is

$$e_{\hat{c}}^{ew} = 0.1667 \frac{\Theta(t; -1.75\tau_0, -1.25\tau_0)}{\tau_0} + 0.3333 \frac{\Theta(t; -1.25\tau_0, 1.25\tau_0)}{\tau_0} + 0.1667 \frac{\Theta(t; 1.25\tau_0, 1.75\tau_0)}{\tau_0}. \quad (16)$$

From equation (12) this gives the force-basis estimating function

$$y_{\hat{c}}^{ew} = 0.1667(1 - \sin(\omega_0 t)) \frac{\Theta(t; -1.75\tau_0, -1.25\tau_0)}{\tau_0} + 0.3333 \frac{\Theta(t; -1.25\tau_0, 1.25\tau_0)}{\tau_0} + 0.1667(1 + \sin(\omega_0 t)) \frac{\Theta(t; 1.25\tau_0, 1.75\tau_0)}{\tau_0}. \quad (17)$$

The variance in the corresponding estimator is 112% of optimum (this numerical result and others from the following discussion will be represented in Figure 3).

To illustrate why the Eöt-Wash estimator is superior to the boxcar estimator (112% of optimum compared with 150%), Figure 1 shows the Eöt-Wash force-basis estimating function as the sum of its parts. In the force basis, the boxcar estimating function is a constant plus a sinusoid whereas the Eöt-Wash estimating function is simply a constant with smooth transitions to zero near the endpoints (sinusoidal profile). As mentioned in the previous section, the optimal estimating function is a boxcar in the force basis—a function more closely approximated by the Eöt-Wash estimator than by a displacement-basis boxcar.

Comparing the 3-period boxcar estimator with a 3.5-period Eöt-Wash estimator is not entirely a fair com-

parison. The variance of a 3-period Eöt-Wash estimator, which results from the sum of two mutually displaced 2.5-period boxcar estimating functions, is 114% of optimum—still significantly better than the boxcar estimator. In addition, while the constituent 2.5-period boxcars are not individually orthogonal to the pendulum oscillation the 3-period Eöt-Wash estimator is. Indeed, any Eöt-Wash estimator is a force-only estimator because the unique summation scheme removes the effect of the free oscillation to zero order in $1/Q$. On the other hand, any boxcar estimator that is a half-integer number of periods in duration will suffer a significant penalty of order Q in variance inflation as shown in Paper I.

If we were to use the Eöt-Wash estimator for a single period of data, then the resulting variance in the parameter estimator would be 150% of the optimum—identical to the variance for the boxcar. This can be seen in Figure 1 where, if the flat middle portion of the force-basis estimating function were to vanish, the remaining function is equivalent to the force-basis representation of the boxcar estimating function, a sinusoid. Thus, within a few periods of data the Eöt-Wash estimator improves dramatically over the boxcar estimator.

The variance in the Eöt-Wash estimator continues to converge toward the optimal estimator as the observation interval increases because the constant portion of the force-basis estimating function constitutes a larger and larger fraction of the total duration. In the force basis, the primary difference between the Eöt-Wash estimator and the optimal estimator is the smooth transition at the edges from the constant value to zero for the former as opposed to the step function transition for the latter. For thermal noise, abrupt edges characterize the optimal estimator; however, the consequence of those edges is shown when white noise, which lacks a high-frequency cutoff, is present. We discuss the effects of these discontinuities in Section III B.

The trigonometric approach, a different, but straightforward improvement of the boxcar estimator, results from including the sine and cosine components of the free oscillation of the pendulum in the fit. This trigonometric approach produces reasonable estimators for any duration of the sample. The 3.5-period estimating functions in the displacement and force bases are then

$$e_{\hat{p}}^{tr} = \frac{\Theta(t; -1.75\tau_0, 1.75\tau_0)}{\tau_0} (0.2905 + 0.0528 \cos(\omega_0 t)) \quad (18)$$

and

$$y_{\hat{p}}^{tr} = \frac{\Theta(t; -1.75\tau_0, 1.75\tau_0)}{2\pi m\omega_0} \times (0.2905 + 0.0264 \cos(\omega_0 t) + 0.0264\omega_0 t \sin(\omega_0 t)) \quad (19)$$

respectively. The variance of the 3.5-period trigonometric estimator is 118% of optimum, much better than 150% for the 3-period boxcar (which is equivalent to the 3-period trigonometric estimator). Not only is this estimator acceptable, but it is superior to the integer period boxcar. Indeed, in terms of variance (not variance

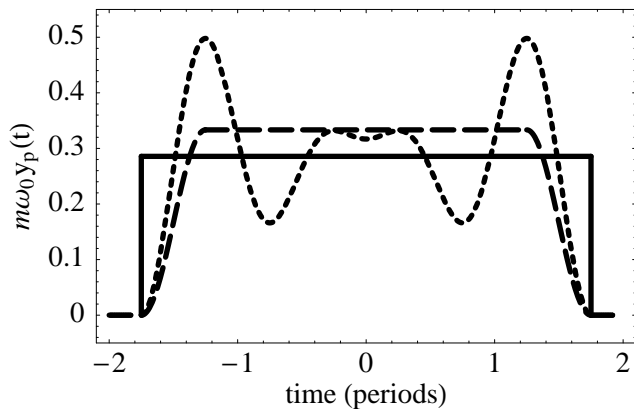


FIG. 2: A comparison of the 3.5-period optimum (solid), Eöt-Wash (dashed), and trigonometric (dotted) force-basis estimating functions.

times time) the 3.5-period trigonometric estimator is better than the 4-period trigonometric estimator.

Although its force-basis estimating function always contains oscillatory terms and does not, therefore, resemble the constant profile of the optimal estimating function, the half-integer period trigonometric estimator is better than its integer period counterpart because there is a triangular envelope on the sine component of the oscillation which suppresses the contribution from that term. Figure 2 overlays the 3.5-period optimum, Eöt-Wash, and trigonometric estimating functions. For longer observation times, the trigonometric estimator remains at 150% of optimum for integer periods and converges to $7/6 = 117\%$ of optimum for half-integer periods, if examined to first order in $1/Q$ —this is unlike the Eöt-Wash estimator which converges identically to the optimum. The top panel of Figure 3 compares the variances in these three estimators multiplied by the duration of the sample for 1, 1.5, 3, 3.5, 9, and 9.5 periods of data.

We take the values of 9 and 9.5 periods, as selected by the Eöt-Wash group, to be representative of practice. Our original choice of examining 3 and 3.5 periods constitute useful samples of intermediate duration, and matches the convention of the Eöt-Wash group to modulate their force at $2/3$ of the resonant frequency[5]. Three periods of data also correspond to the first choice for which both an integer number of modulation periods and an integer number of pendulum oscillation periods occur. The 3.5-period results are shown because the Eöt-Wash convention uses raw data that spans a half-integer number of periods.

Since the variance in the Eöt-Wash estimator approaches that in the optimal estimator as the duration of the data increases, a practical limit to the length of the observations is set primarily by factors that lie beyond mathematical considerations. These could include unavoidable non-Gaussian disturbances that partition the realization or low-frequency noise (drift).

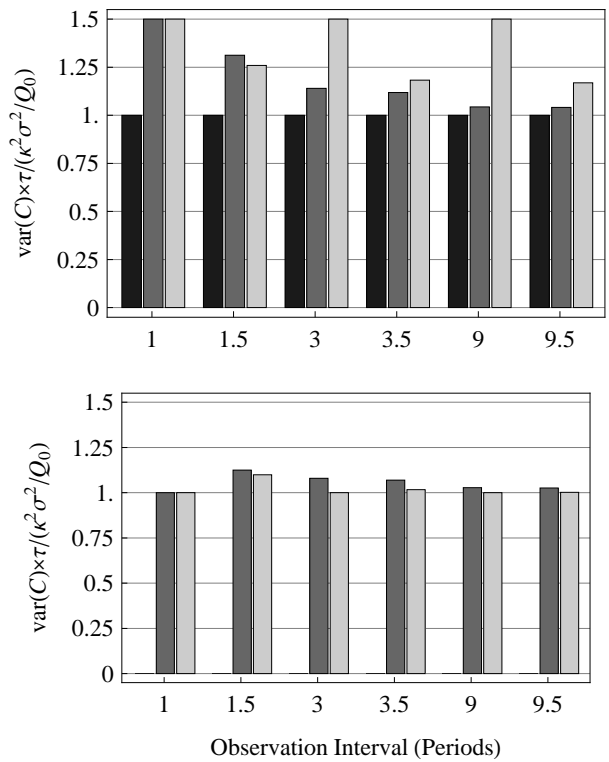


FIG. 3: Comparison of variances in the optimal estimator (black), Eöt-Wash estimator (dark gray), and the trigonometric estimator (light gray) in the presence of thermal noise (top panel) and white noise (bottom panel) for observation intervals equal to 1, 1.5, 3, 3.5, 9, and 9.5 oscillation periods. For white noise, the variance in the optimal thermal noise estimator would be infinite and is therefore not shown. Here, the white noise PSD is normalized to match the zero frequency limit of the thermal noise PSD [see equation (21)]

B. White Noise and Mixed Noise

So far we have examined only the effects of thermal noise on the variances in these estimators. A real system will always display some white displacement noise as well. For white noise the variance of a given parameter estimator is most easily obtained in the displacement basis

$$\text{var}(\hat{P}_{wh}) = \frac{\eta}{2} \int_{-\infty}^{\infty} e_p^2 dt \quad (20)$$

where η is the (constant) PSD of the noise. Since the displacement-basis estimating functions involve derivatives of the force-basis estimating functions (see equation (9)), only those force-basis estimating functions that are smooth (i.e. second-order differentiable) will have a well defined variance in the presence of white displacement noise. The step-function transition exhibited by the estimating functions that are optimal for thermal noise will have Dirac delta functions and their derivatives in the displacement basis. Thus, the high-frequency components of white noise are infinitely amplified by those

TABLE I: Noise mixing ratios for various sample durations where the trigonometric estimators become superior to the Eöt-Wash estimators. The Eöt-Wash estimators are superior when the white noise contribution is less than the stated amount.

Periods	3	3.5	9	9.5
White Noise Fraction	82%	55%	94%	84%

delta functions and the variances of the estimators diverge to infinity.

The lower panel of Figure 3 displays the variances in each of the two approximate estimators for the case of white noise. For comparison, we normalize the white noise PSD so that it is equal to the zero frequency limit of the thermal noise PSD. That is,

$$\begin{aligned}
 S[\delta X_{wh}(t); \nu] &= S[\delta X_{th}(t); \nu = 0] \\
 &= \frac{4k_B T \xi}{\kappa^2} \\
 &= \frac{4\sigma^2}{Q_0 \omega_0}.
 \end{aligned} \tag{21}$$

We see from Figure 3 that the trigonometric approach is always superior to the Eöt-Wash approach for the case of white noise, although the difference may be small.

The optimal estimator for white displacement noise is the boxcar estimator. Both the trigonometric and the Eöt-Wash estimators are equivalent to the boxcar estimator for a single period of data, as can be seen in both panels of Figure 3. For 1.5 periods, the trigonometric estimator has smaller variance than the Eöt-Wash estimator for both noise processes. As the duration increases, however, the Eöt-Wash estimator performs better than the trigonometric estimator for thermal noise.

From the calculations in this section we can do more than qualitatively compare the two approximate estimators; we can identify the ratio of white to thermal noise where one approach becomes superior to the other. Following the PSD normalization in equation (21), we state the mixing ratios as the fraction of the total noise power contributed from a given noise process, white or thermal. Table I outlines the results of this test.

These results indicate that a knowledge of the dominant noise components and their relative importance is a necessary ingredient informing the choice of the data acquisition protocol, sample duration, and the parameter estimation technique to be applied. Moreover, an intuitive understanding of how the general shape of an estimating function depends upon sample duration—and consequently affects the estimator variance (see Figures 1 and 2)—may prove a valuable guide when confronted with realistic noise backgrounds or further modifications to the noise PSD. As an example, we later explore the case for thermal noise with a $1/f$ PSD where we apply the ideas discussed here.

IV. FIT FOR MULTIPLE PARAMETERS

We now give a brief review of linear, optimal, multi-parameter fits for discrete data, which we then generalize to include fits to a continuous time series. For white noise the techniques for discrete data are readily extended to continuous data because the data covariance matrix is a multiple of the identity matrix and thus can be trivially inverted. For thermal noise, the generalization from discrete to continuous requires that we develop an equivalent formulation of the discrete case that relies on knowledge of the optimal single-parameter filters, which we derive in Paper I, rather than an explicit inversion of the data covariance matrix.

A. Linear Multi-Parameter Fits for Discrete Data

For a multi-parameter fit with discrete data, the data from a particular realization are assembled into a data vector and the parameters into a parameter vector

$$\begin{aligned}
 \mathbf{x} &= \{x_1, x_2, \dots, x_n\} \\
 \mathbf{p} &= \{p_1, p_2, \dots, p_m\}.
 \end{aligned} \tag{22}$$

Following the convention of Paper I, the true, physical value of the parameters will be specified by the vector $\boldsymbol{\rho}$. The partial derivatives of the data with respect to each of the parameters constitutes the design matrix, $\overline{\mathbf{q}}$. To avoid confusion between vectors and matrices, matrices will be indicated by an overbar. The data vector can then be decomposed into a signal vector, the product of the design matrix with the physical parameter vector, and a noise vector $\delta\mathbf{x}$ which is a realization of the random vector $\delta\mathbf{X}$

$$\mathbf{x} = \overline{\mathbf{q}} \boldsymbol{\rho} + \delta\mathbf{x}. \tag{23}$$

The noise covariance matrix

$$\overline{\mathbf{m}}_X = \langle \delta\mathbf{X} \otimes \delta\mathbf{X} \rangle. \tag{24}$$

characterizes the second moments of the noise ensemble, and a parameter estimate vector is obtained by contracting an estimating matrix $\overline{\mathbf{e}}_{\hat{\mathbf{p}}}$ with the data vector,

$$\hat{\mathbf{p}} = \overline{\mathbf{e}}_{\hat{\mathbf{p}}} \mathbf{x}. \tag{25}$$

Many books (see e.g. Hamilton [6]) develop the general theory of optimal, least-squares, parameter estimation for discrete data. Here we simply quote one of the main results. The optimal estimating matrix that returns the minimum variance estimate of all parameters in the presence of the noise $\delta\mathbf{X}$ is

$$\overline{\mathbf{e}}_{\hat{\mathbf{p}}}^{op} = (\overline{\mathbf{q}}^T \overline{\mathbf{m}}_X^{-1} \overline{\mathbf{q}})^{-1} \overline{\mathbf{q}}^T \overline{\mathbf{m}}_X^{-1} \tag{26}$$

We also note that the design matrix and the optimal estimating matrix are pseudo-inverses. That is

$$\overline{\mathbf{e}}_{\hat{\mathbf{p}}}^{op} \overline{\mathbf{q}} = (\overline{\mathbf{q}}^T \overline{\mathbf{m}}_X^{-1} \overline{\mathbf{q}})^{-1} \overline{\mathbf{q}}^T \overline{\mathbf{m}}_X^{-1} \overline{\mathbf{q}} = \mathbf{I}. \tag{27}$$

If this orthonormality condition were not met, a bias would be present in the parameter estimates.

B. Optimal White Noise Multi-Parameter Fit for Continuous Data

Although the Eöt-Wash method pre-filters the data and the trigonometric method adds two additional parameters, both methods ultimately fit the data in the manner that is optimal for white noise. Thus it is instructive to consider optimal, white noise, multi-parameter fits in the continuous limit. For discrete white noise fits, the data covariance matrix is a multiple of the identity matrix, and the optimal multi-parameter estimating matrix in (26) simplifies to

$$\bar{\mathbf{e}}_p^{op} = (\bar{\mathbf{q}}^T \bar{\mathbf{q}})^{-1} \bar{\mathbf{q}}^T. \quad (28)$$

The transition from discrete to continuous data is then straightforward—the design matrix becomes a vector of functions that is multiplied by the parameter vector to produce the multi-parameter signal. Thus,

$$x(t; \mathbf{p}) = \mathbf{q}(t) \cdot \mathbf{p}. \quad (29)$$

The estimating matrix becomes a vector of functions such that

$$\hat{\mathbf{p}} = \int_{-\infty}^{\infty} \mathbf{e}_p(t) x(t) dt. \quad (30)$$

The design vector and the optimal estimating vector of functions satisfy the orthonormality condition,

$$\int_{-\infty}^{\infty} \mathbf{e}_p^{op}(t) \otimes \mathbf{q}(t) dt = \mathbf{I} \quad (31)$$

where \otimes represents an outer product.

In analogy with the discrete white noise case, the optimal estimating functions are obtained from the vector of design functions,

$$\mathbf{e}_p^{op}(t) = \left(\int_{-\infty}^{\infty} \mathbf{q}(t) \otimes \mathbf{q}(t) dt \right)^{-1} \mathbf{q}(t) \quad (32)$$

This equation essentially states that the optimal white noise estimating functions are linear combinations of the single-parameter matched filters such that the estimating functions are orthogonal to the design functions of the remaining parameters[6].

C. Optimal Thermal Noise Multi-Parameter Fit for Continuous Data

We now look at an alternative formulation of the discrete fit that does not use an explicit inversion of the data covariance matrix. This formulation is desirable when considering continuous data, since inverting the covariance matrix would require finding the Green's function that diagonalizes the covariance operator. Avoiding this step simplifies the calculations.

Consider the case of a single-parameter fit to discrete data. The design matrix and estimating matrix are then vectors. The optimal estimating matrix

$$\mathbf{e}_p^{op} = (\mathbf{q} \bar{\mathbf{m}}_X^{-1} \mathbf{q})^{-1} \mathbf{q} \bar{\mathbf{m}}_X^{-1} \quad (33)$$

is also a vector and the term $(\mathbf{q} \bar{\mathbf{m}}_X^{-1} \mathbf{q})^{-1}$ is a multiplicative constant. From this result, we define the optimal single-parameter filter,

$$\mathbf{f}_p^{op} = \mathbf{q} \bar{\mathbf{m}}_X^{-1} \quad (34)$$

and allow the constant mentioned before to assume the role of normalization.

To extend this to multi-parameter fits, let us provisionally define an optimal multi-parameter filter matrix as

$$\bar{\mathbf{f}}_p^{op} \equiv \bar{\mathbf{q}}^T \bar{\mathbf{m}}_X^{-1} \quad (35)$$

where each row of the filter matrix is the optimal single-parameter filter for the corresponding parameter. In addition, let us assume that the optimal estimating matrix can be obtained from this filter matrix through multiplication by some square matrix $\bar{\mathbf{n}}$. Since the optimal estimating matrix and the design matrix are pseudo-inverses

$$\bar{\mathbf{e}}_p^{op} \bar{\mathbf{q}} = \bar{\mathbf{n}} \bar{\mathbf{f}}_p^{op} \bar{\mathbf{q}} = \mathbf{I} \quad (36)$$

the matrix $\bar{\mathbf{n}}$ must have the value,

$$\bar{\mathbf{n}} = \left(\bar{\mathbf{f}}_p^{op} \bar{\mathbf{q}} \right)^{-1}. \quad (37)$$

Examination of equation (36) shows that the estimating matrix is

$$\bar{\mathbf{e}}_p^{op} = \bar{\mathbf{n}} \bar{\mathbf{f}}_p^{op} = (\bar{\mathbf{q}}^T \bar{\mathbf{m}}_X^{-1} \bar{\mathbf{q}})^{-1} \bar{\mathbf{q}}^T \bar{\mathbf{m}}_X^{-1}, \quad (38)$$

in agreement with the optimal estimating matrix (26). Thus, our assumption that $\bar{\mathbf{e}}_p^{op} = \bar{\mathbf{n}} \bar{\mathbf{f}}_p^{op}$ is seen to be justified. Moreover, we now have an equation for the optimal estimating matrix

$$\bar{\mathbf{e}}_p^{op} = \left(\bar{\mathbf{f}}_p^{op} \bar{\mathbf{q}} \right)^{-1} \bar{\mathbf{f}}_p^{op}, \quad (39)$$

which does not require knowledge of $\bar{\mathbf{m}}_X^{-1}$.

This form can now be taken to the continuous limit. The vector of optimal estimating functions is obtained from the vector of single-parameter filters and the vector of design functions.

$$\mathbf{e}_p^{op}(t) = \left(\int_{-\infty}^{\infty} \mathbf{f}_p^{op}(t) \otimes \mathbf{q}(t) dt \right)^{-1} \mathbf{f}_p^{op}(t) \quad (40)$$

Similar to the white noise case, this demonstrates the important result that the optimal thermal noise estimating functions are linear combinations of the optimal, single-parameter filters. We apply this information to a multi-parameter model and study its consequences in the next section.

V. FIT TO A FOUR PARAMETER MODEL

The results from this article as well as from our previous work are valid for a constant-force signal. As stated in the introduction, such a signal is indistinguishable from the normal equilibrium displacement of the oscillator. To break this degeneracy one must modulate the force signal. We maintained in our previous work that our constant-force results were readily applicable to modulated signals; we now refine that assertion.

We choose to modulate the force signal at $2/3$ the oscillation frequency $\omega_s = 2/3\omega_0$ —a modulation frequency that is commonly employed by the Eöt-Wash group. For this choice of ω_s , the displacement amplitude is a factor of

$$\frac{1}{1 - (\omega_s/\omega_0)^2} = \frac{9}{5} \quad (41)$$

larger than for a stationary force of the same magnitude. This raises the question of whether we should compare the constant force results to a modulated signal of the same displacement amplitude or the same driving force amplitude. The answer to this question depends upon the experimental approach that one employs for a given experiment. For a torsion balance experiment using a turntable to modulate the signal frequency, it is the magnitude of the applied force that remains constant as the modulation frequency increases. Thus, a comparison of equivalent driving force amplitude provides a more useful comparison of signal-to-noise ratio.

We parameterize the oscillator's response as

$$x(t) = \frac{9}{5} \frac{a_s}{\kappa} \cos(\omega_s t) + \frac{9}{5} \frac{b_s}{\kappa} \sin(\omega_s t) + c_0 + c_1 t \quad (42)$$

so the variance in signal parameters a_s and b_s reflects the same uncertainty in the applied force as an equivalent variance in the c parameter introduced in the earlier, single-parameter sections. We rename c as c_0 , which corresponds to the equilibrium displacement of the pendulum mass in the absence of the external force, and we add the parameter c_1 to account for a linear drift in the equilibrium displacement, which commonly occurs as the torsion fiber relaxes.

A. Modulated Signal and Thermal Noise

With the mathematical tools presented in the previous section we calculate the variance of the optimal, multiparameter estimators for the signal parameters a_s and b_s when accounting for thermal noise exhibited by the oscillator. We compare those variances with the variances of the estimators from the trigonometric and Eöt-Wash approaches. The results of these calculations for 3, 3.5, 9 and 9.5 periods are given in Figure 4.

We see in Figure 4 that modulating the signal causes the optimal thermal noise variance to be roughly a factor of two larger than the variance for the constant force estimator. This factor of two could be recovered if the force

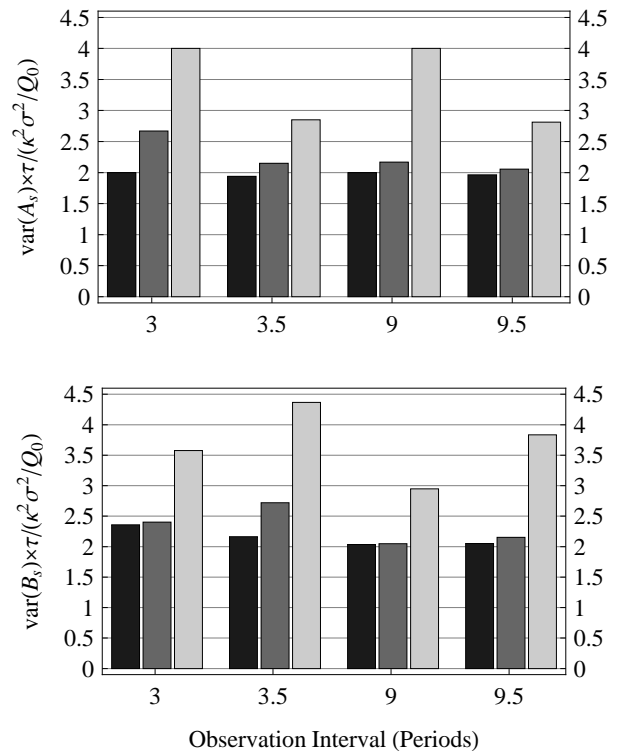


FIG. 4: Comparison of the estimator variances for cosine (top) and sine (bottom) signal amplitudes for the multiparameter fit (see equation (42)) using the optimal thermal noise estimator, the Eöt-Wash estimator, and the trigonometric estimator in the presence of thermal noise. The grayscale convention is the same as in Figure 3.

were modulated as a square wave instead of a sinusoid—a technique occasionally implemented [7, 8]. Regardless, sinusoidal modulation offers the advantage of simultaneously measuring both quadrature components of the signal. Thus, if one requires knowledge of both of these parameters, then no measurement time is lost. Moreover, sinusoidal modulation of the signal can help reject gravitational systematics with higher azimuthal symmetries (such as $\cos(3\omega_s t)$ or $\sin(3\omega_s t)$).

When fitting these parameters optimally for thermal noise, the variances of the several sine amplitude estimators are larger than those of the cosine amplitudes. This effect can be attributed to two factors. First, there is greater functional overlap between the b_s and c_1 parameters compared to that between a_s and c_0 . Second, for half-integer periods, the total energy of the sine signal is slightly less than that of the cosine signal. This fact is not surprising as the same effects arise for the case of the optimal white noise fit to these same four parameters. Indeed, the variances of the optimal thermal noise estimators are identical to those of the optimal white noise estimators without the factor of $9/5$ in the expressions for a_s and b_s , and with the “equivalent” white noise power defined as in equation (21) of Section III B.

To see why this is so, let us first denote the optimal white estimator in the presence of white noise with the

subscript “ I ” and the optimal thermal noise estimator in the presence of thermal noise with the subscript “ II ”. The component functions of the design vector for the optimal white-noise fit are then, $\mathbf{q}_I(t) = \{\cos(\omega_s t), \sin(\omega_s t), 1, t\}$. For the optimal thermal-noise fit (factors of 9/5 included) they are $\mathbf{q}_{II}(t) = \{9/5 \cos(\omega_s t), 9/5 \sin(\omega_s t), 1, t\}$. The stated equivalence arises because the four functions of $\mathbf{q}_{II}(t)$ in the driving-force basis are directly proportional to the four functions of $\mathbf{q}_I(t)$ in the displacement basis. That is, to zero-order in $1/Q$,

$$\Omega[\mathbf{q}_{II}(t)] = \kappa \mathbf{q}_I(t). \quad (43)$$

Since all four components of $\mathbf{q}_{II}(t)$ are non-zero, it can be shown that the optimal estimators for thermal noise must be force-only, and that they may be calculated in the driving-force basis. Specifically there would be an analog to equation (32) in Section IV with $\bar{\mathbf{e}}_p^{op}$ replaced with $\bar{\mathbf{y}}_p^{op}$ and with $\mathbf{q}(t)$ replaced with $\Omega[\mathbf{q}(t)]$. From this, one then gets

$$\bar{\mathbf{y}}_{pII}^{op} = \bar{\mathbf{e}}_{pI}^{op}/\kappa. \quad (44)$$

From equation (21), one notes a distinguishing factor of κ^2 between the driving-force PSD of II , $4k_B T \xi$, and the displacement PSD of I . When calculating the variances in the parameter estimates, all of these factors of κ cancel, yielding identical values for both the optimal white estimator with white noise and the optimal thermal estimator with thermal noise.

For the Eöt-Wash estimators, pre-filtering the data leads one to ask whether the signal amplitude is thereby reduced by a factor of two. In fact, it is; however, the noise is also filtered. For a long data duration the FED is narrowbanded around the signal frequency and the ratio of the attenuation in the signal and the attenuation in the noise is very nearly unity. In this manner, the Eöt-Wash estimator approaches the optimum just as it did for the static case discussed in Section III A. In essence, this argument is the Fourier representation of that discussion.

Unlike the Eöt-Wash estimators, the trigonometric estimators do not converge to the optimum for a modulated signal. The narrowbanding argument from the previous paragraph does not apply for the trigonometric estimators because a significant contribution from the resonance frequency is required in order to match the necessary boundary conditions of a force-only estimator—that it have smooth transitions to zero. This effect does not occur just at the beginning and end of the data, and thus its contribution does not diminish to zero with longer duration measurements.

The DC-signal trigonometric estimators discussed in Section III may provide a good qualitative understanding of the modulated-signal trigonometric estimators in this section. However, a comparison of Figures 3 and 4 show important quantitative differences in the estimator variances between the modulated and static cases. For example, a common assumption that the DC signal is a special case of the cosine component of the modulated signal proves incorrect as the variance of the cosine amplitude is larger than optimum by a factor of two instead

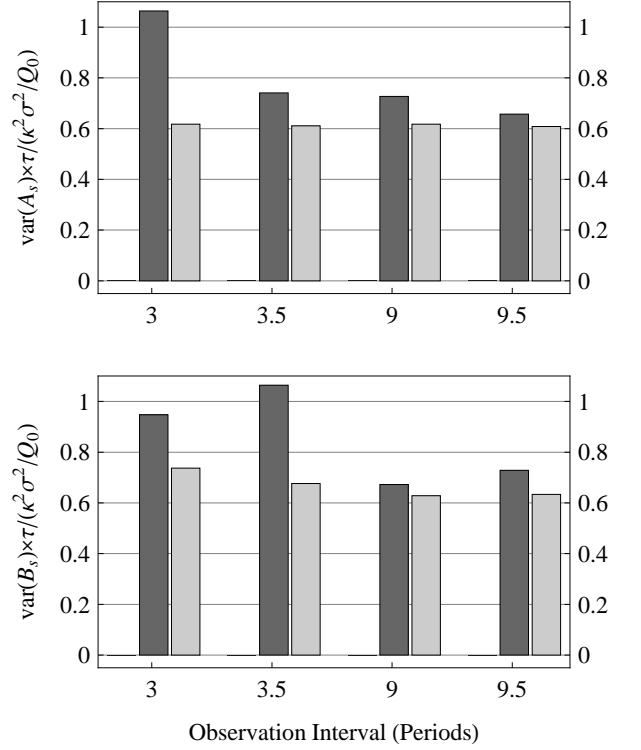


FIG. 5: Comparison of the estimator variances for cosine (top) and sine (bottom) signal amplitudes for the multiparameter fit (see equation (42)) using the Eöt-Wash estimator and the trigonometric estimator in the presence of white noise. The grayscale convention is the same as in Figure 3.

the factor of 3/2 for the static case of Section III. Thus, a specific calculation of the estimator variances is required to achieve reliable numerical results for a modulated signal.

B. Modulated Signal and White Noise

The white-noise counterparts to the thermal-noise results in Figure 4 are shown in Figure 5. The estimator variances in the presence of white noise are generally a factor of $(5/9)^2$ smaller than the corresponding estimators in the presence of thermal noise. This follows because the displacement basis signal becomes 9/5 larger while the additive noise remains the same. For thermal noise, the response of the oscillator causes both signal and noise to increase by the same factor, leaving the signal-to-noise ratio unchanged.

The trigonometric estimators are nearly optimal in the presence of white noise because they are, in essence, optimal white-noise fits but with two additional terms, $a_0 \cos(\omega_0 t)$ and $b_0 \sin(\omega_0 t)$. The differences from the optimal case are due to the functional overlap of a_0 and b_0 with the other four parameters. Since these overlaps tend to decrease as the data duration increases, the trigonometric estimators converge to the optimum.

When compared with the optimal estimators for either

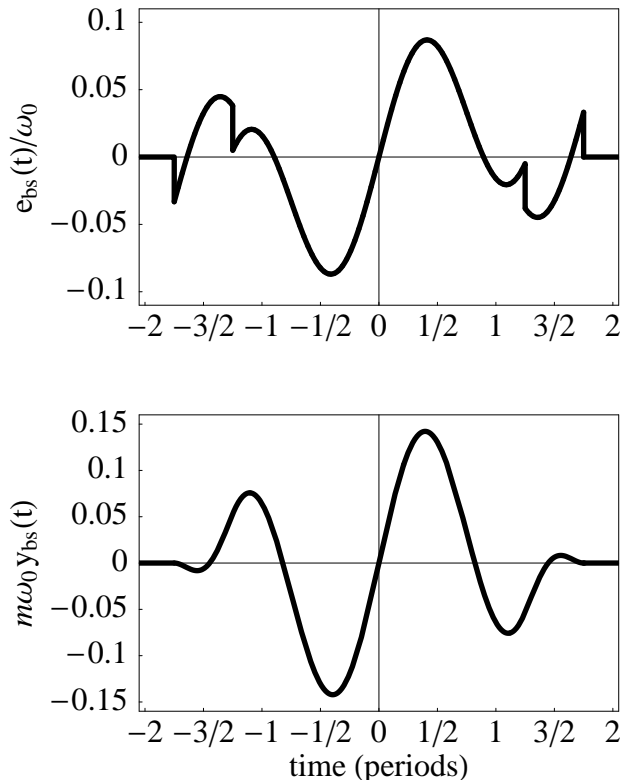


FIG. 6: Comparison of the e_p (top) and y_p (bottom) for the Eöt-Wash estimator for the 3.5-period sine amplitude. The jump discontinuities that are present in the e_p give the Eöt-Wash estimators larger variance than the trigonometric estimators in the presence of white displacement noise. For thermal noise the same does not occur because, in the basis where the thermal driving force is white and the y_p is used, there are no such discontinuities.

noise process, the Eöt-Wash estimators are much closer to optimum for thermal noise than they are for white noise. The reason for this behavior is subtle, as the argument for high performance of Eöt-Wash estimators in the presence of thermal noise—that the central portion of the y_p 's approximate matched filters well, and only the first and last quarter periods deviate significantly from optimal—would seem to apply just as well to the estimating functions in the displacement basis that are used to calculate the white noise variances. The reason for the difference becomes clear in Figure 6. By comparing the e_p and y_p for the sine amplitude in the 3.5-period trigonometric estimator we see that, by construction, the e_p has jump discontinuities. The y_p , on the other hand, is obtained through a convolution of the e_p (see equation (12) in Section II) and therefore must be a continuous function. The e_p , with its jump discontinuities, is thus more free to deviate from an optimal matched filter. Thus, the Eöt-Wash estimator performs less well in the presence of white noise.

TABLE II: Noise mixing ratios for various sample durations where the trigonometric estimators become superior to the Eöt-Wash estimators for the four-parameter model discussed. The Eöt-Wash estimators are superior when the white noise contribution is less than the stated amount.

Periods	3	3.5	9	9.5
White Noise Fraction	79%	82%	95%	94%

C. Mixed Noise

What about mixed noise and multiparameter fits? For a modulated signal and with the addition of the polynomial parameters c_0 and c_1 , we can identify the ratios of thermal to white noise where the Eöt-Wash estimation technique gives equal variances to the trigonometric approach as done in Section III B. These results are given in table II.

For a measurement scheme in which white noise dominates, the experimenter should likely consider increasing the modulation frequency closer to resonance in an effort to increase the signal-to-noise ratio (the signal-to-noise ratio for thermal noise is independent of the modulation frequency). In such a situation a resonant method would be suitable. With some modification to accommodate non-linear fits, the techniques developed in this article can be applied to resonant and other large-oscillation-amplitude detection schemes [8, 9] though a detailed exploration of that topic lies beyond the scope of this work.

D. 1/f Thermal Noise

For modern torsion balance experiments that are conducted at high vacuum, the predominant damping/noise mechanism is the fiber dissipating energy rather than residual gas in the vacuum chamber. Saulson [10] states that for this scenario a $1/f$ profile is a better approximation to the driving force PSD than the white driving force that is characteristic of a classical dashpot. Mathematically, such a spectrum is less tractable, so there is no simple method for finding the optimal estimating functions as for the oscillator with dashpot damping.

Nevertheless, we can still calculate and compare the variances of our estimating functions. We compute these quantities in the driving force basis since it is still easier than in the displacement basis, but we must now numerically integrate the product of the PSD and the FED (see equation (2)). We first note that this revised damping of the oscillator is frequency dependent with a functional form similar to that of the driving force:

$$\xi(\nu) = \frac{\xi_0 \nu_0}{\nu}. \quad (45)$$

where $\nu_0 = \omega_0/(2\pi)$ is the resonance frequency (in Hz) and ξ_0 is the velocity damping coefficient that corresponds to the resonance frequency. This form constrains the observed damping at the resonance frequency to be

the same for both $1/f$ thermal noise and for dashpot thermal noise.

The variance in the parameter estimators for $1/f$ noise is then

$$\begin{aligned}\text{var}(\hat{P}_{1/f}) &= \frac{1}{2} \int_0^\infty F^2[y_{\hat{p}}] S[\Omega[\delta X_{1/f}]] d\nu \\ &= \frac{1}{2} \int_0^\infty F^2[y_{\hat{p}}] [4k_B T \xi(\nu)] d\nu \\ &= 2k_B T \xi_0 \int_0^\infty F^2[y_{\hat{p}}] \frac{\nu_0}{\nu} d\nu.\end{aligned}\quad (46)$$

Here the $1/f$ subscript signifies that the driving force PSD has a $1/f$ profile.

The zero-frequency PSD singularity for $1/f$ noise requires the FED of the parameter estimating function $F^2[y_p]$ to have a corresponding zero in order for the variance to be well defined. That is, y_p must be orthogonal to a constant force signal. The estimating functions for a_s and b_s are orthogonal to the constant signal parameterized by c_0 , and since they are force-only estimators, it can be shown that their corresponding y_p 's are also orthogonal to a constant. Thus, the variance of the estimators for a_s and b_s remain finite. The variances for all three methods—optimal thermal, Eot-Wash, and trigonometric—are shown in Figure 7 for different observation intervals. Once again, the signal frequency, $\omega_s = 2/3\omega_0$.

Comparing variance in the optimal thermal noise estimator for the case of $1/f$ thermal noise (Figure 7) with dashpot thermal noise (Figure 4) we see that the variance with $1/f$ noise is larger by about 50%. This is largely because that noise is greater by 50% at the chosen signal frequency. We also see from Figure 7 that the optimal thermal noise estimator is actually slightly inferior to the Eöt-Wash estimator for some values of the sample duration. Consequently, the optimal thermal noise estimator is not the true optimal estimator for $1/f$ thermal noise. However, a comparison of the results for $1/f$ thermal noise in Figure 7 with the results of both dashpot thermal noise in Figure 4 and white displacement noise in Figure 5, shows that dashpot thermal noise is a better model to guide the choice of an estimator for $1/f$ thermal noise.

VI. DISCUSSION

The topics discussed in this paper illustrate the differences between existing parameter estimation techniques relative to the optimum technique for thermal noise dominated experiments. A major simplification in the study and application of parameter estimation for this case results from working in the basis of the thermal driving force where the PSD of the noise is white. Equations (9) and (12) show how to transform between the displacement basis and the driving-force basis.

In the driving-force basis, analysis practices that are commonly applied to data exhibiting white displacement noise can be utilized for estimation in the presence of

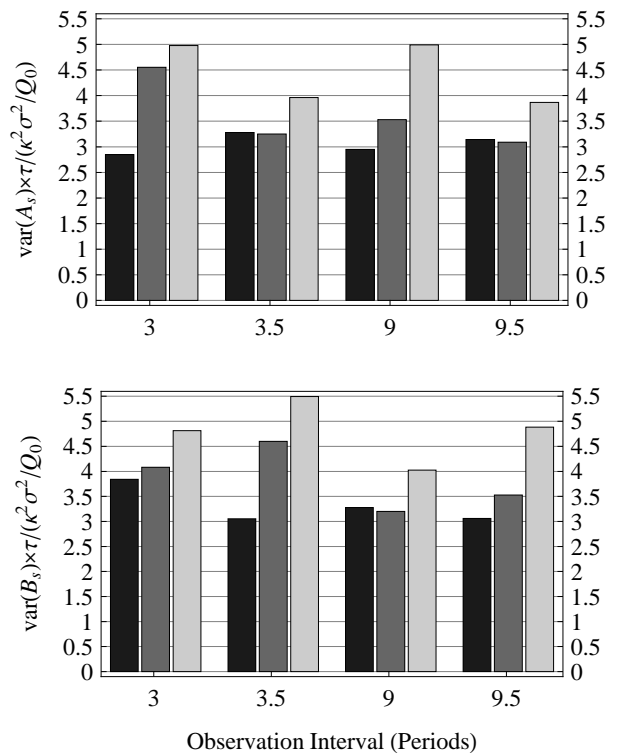


FIG. 7: Comparison of the estimator variances for cosine (top) and sine (bottom) signal amplitudes for the multiparameter fit (see equation (42)) using the optimal thermal noise estimator, Eöt-Wash estimator and the trigonometric estimator in the presence of $1/f$ noise. The grayscale convention is the same as in Figure 3.

thermal noise. Working in that basis allows clearer insight to the efficacy of the various approximate methods that experimentalists generally employ. Additionally, working in the driving force basis ensures that a parameter estimator is insensitive to the effects of the resonance peak. As discussed in Paper I, this feature also provides immunity to transient oscillations induced by disturbances that occur prior to the data sample. A further advantage, for modulated signals, is that the signal frequency does not have to be commensurate with the natural oscillation frequency. In fact, there can be two or more signal frequencies that need not be commensurate with each other.

While the approach we outline may be applied generally, the interesting calculations can be truncated to leading order in $1/Q$ without losing value to an experimentalist. Specifically, meaningful results are obtained—and with greater facility—using the undamped approximation for the signal and estimating functions. Besides making analytic calculations simpler, working in the driving-force basis makes leading-order numerical solutions more robust against artificial influence of power from the resonance peak.

For a real torsion pendulum experiment, the superposition of several noise processes is a challenge that requires one to adopt a data analysis scheme that performs

well under a variety of circumstances, while necessarily being optimal in none. We have shown that the estimation technique used by the Eöt-Wash group is not only well behaved in the presence of white displacement noise, thermal noise, and $1/f$ noise but approaches the performance of the optimum for both white and thermal noise as the duration of the observations increase. For $1/f$ noise, the Eöt-Wash estimator also performs well relative to the other techniques studied in this paper, though the singular nature of $1/f$ noise renders identifying its corresponding optimal estimators intractable. By using the dashpot thermal noise results as a guide, one can correctly infer that the Eöt-Wash estimator is superior to the trigonometric estimator for $1/f$ thermal noise; whereas if one had used the white noise results as a guide, one might erroneously assume the trigonometric estimator to be superior.

Even with the mathematical tools developed here and in Paper I, there remain several issues that are important to a modern experimental research that lie beyond the scope of this work. One obvious example is our *a priori* assumption regarding knowledge of the oscillation frequency and quality factor of the pendulum. Ideally one would like to identify these quantities from the same data used to estimate the other parameters of the system—

especially if the experiment uses a pendulum that undergoes large amplitude oscillations. Moreover, for extension to the case of large amplitude oscillations, the nonlinear nature of both the oscillation frequency and the decay constant require an additional generalization of the techniques discussed here. This is even true of the linear signal parameters of non-resonant, higher harmonic methods, such as the treatment of the second harmonic we employ in our own experiments because signal-to-noise ratio considerations still require operation with large-amplitude oscillations [1]. We leave for further investigation the optimal estimation of multiple, nonlinear parameters and its implications for torsion pendulum experiments.

Acknowledgments

We gratefully acknowledge NSF Grants PHY- 0244762, -060692, and -071923 for support of this work. JHS recognizes the generous support of the Brinson Foundation and Fermilab under DOE contract No. DE-AC02-07CH11359.

-
- [1] P. E. Boynton, *Classical and Quantum Gravity* **17**, 2319 (2000).
 - [2] C. D. Hoyle, D. J. Kapner, B. R. Heckel, E. G. Adelberger, J. H. Gundlach, U. Schmidt, and H. E. Swanson, *Phys. Rev. D* **70**, 042004 (2004), arXiv:hep-ph/0405262.
 - [3] M. W. Moore, J. H. Steffen, and P. E. Boynton, *Review of Scientific Instruments* **76**, 5106 (2005), arXiv:physics/0412102.
 - [4] Y. Su, B. R. Heckel, E. G. Adelberger, J. H. Gundlach, M. Harris, G. L. Smith, and H. E. Swanson, *Phys. Rev. D* **50**, 3614 (1994).
 - [5] J. H. Gundlach, G. L. Smith, E. G. Adelberger, B. R. Heckel, and H. E. Swanson, *Physical Review Letters* **78**, 2523 (1997).
 - [6] W. C. Hamilton, *Statistics in physical science. Estimation, hypothesis testing, and least squares* (New York: Ronald Press, 1964, 1964).
 - [7] J. K. Hoskins, R. D. Newman, R. Spero, and J. Schultz, *Phys. Rev. D* **32**, 3084 (1985).
 - [8] R. Cowsik, N. Krishnan, S. N. Tandon, and S. Unnikrishnan, *Physical Review Letters* **64**, 336 (1990).
 - [9] P. E. Boynton, R. M. Bonicalzi, A. M. Kalet, A. M. Kleczewski, J. K. Lingwood, K. J. McKenney, M. W. Moore, J. H. Steffen, E. C. Berg, W. D. Cross, et al., *New Astronomy Review* **51**, 334 (2007), arXiv:gr-qc/0609095.
 - [10] P. R. Saulson, *Fundamentals of interferometric gravitational wave detectors* (Singapore: World Scientific Publishers, 1994, xvi, 299 p. ISBN 9810218206, 1994).